Parathyroid Imaging with Simultaneous Acquisition of 99mTc-Sestamibi and 123I: The Relative Merits of Pinhole Collimation and SPECT/CT

Paraag R. Bhatt[1], William C. Klingensmith III[1], Brian M. Bagrosky[1], Jacob C. Walter[1], Kim K. McFann[2], Robert C. McIntyre, Jr.[3], Christopher D. Raeburn[3], and Phillip J. Koo[1]

[1]Division of Nuclear Medicine, Department of Radiology, University of Colorado School of Medicine, Aurora, Colorado; [2]Department of Biostatistics and Informatics, Colorado School of Public Health, Aurora, Colorado; and [3]Division of GI, Tumor and Endocrine Surgery, Department of Surgery, University of Colorado School of Medicine, Aurora, Colorado

The objective of this study was to determine the relative utility of 3 state-of-the-art parathyroid imaging protocols: single-time-point simultaneous acquisition of 99mTc-sestamibi and 123I images with pinhole collimation in the anterior and bilateral anterior oblique projections, single-time-point simultaneous acquisition of 99mTc-sestamibi and 123I images with SPECT/CT, and the combination of the first and second protocols. **Methods:** Fifty-nine patients with surgical proof of parathyroid adenomas were evaluated retrospectively. All 3 protocols included perfectly coregistered subtraction images created by subtracting the 123I images from the 99mTc-sestamibi images, plus an anterior parallel-hole collimator image of the neck and upper chest. The pinhole protocol was performed first, followed by the SPECT/CT protocol. Three image sets were derived from each study in each patient according to the above protocols. Two experienced observers recorded the size, location, and degree of certainty of any identified lesion. **Results:** The 59 patients had 61 adenomas. For the 2 observers combined, the localization success rate was 88% for the pinhole protocol, 69% for the SPECT/CT protocol, and 81% for the combined protocol. The pinhole protocol detected more adenomas than the SPECT/CT protocol and missed fewer adenomas than either the SPECT/CT protocol or the combined pinhole and SPECT/CT protocol (P < 0.01). The 2 protocols that included SPECT/CT provided superior anatomic information relative to the location and size of the parathyroid adenomas. **Conclusion:** The pinhole protocol localized significantly more adenomas than the SPECT/CT protocol. However, the protocols that included SPECT/CT provided more anatomic information than pinhole imaging alone.

Key Words: camera-based high energy imaging; endocrine; SPECT/CT; I-123; parathyroid imaging; pinhole collimation; Tc-99m-sestamibi

Hyperparathyroidism is a relatively common condition, with an incidence of approximately 1 per 1,000 adults (1). At least 80% of cases of hyperparathyroidism are caused by 1 or occasionally more parathyroid adenomas. Most of the remaining cases of hyperparathyroidism are secondary and are caused by renal insufficiency. Preoperative identification and localization of the adenomas allow the surgeon to perform image-guided minimally invasive surgery with improved success rates, shorter operating times, and less morbidity (2). Consequently, it is important to optimize the accuracy of preoperative imaging in determining the presence, size, and location of parathyroid adenomas.

A wide variety of nuclear medicine protocols have been reported for imaging parathyroid glands. The protocols vary depending on whether pinhole or parallel-hole collimation is used, whether SPECT tomography with or without CT is used, whether 1 or 2 radiopharmaceuticals with or without simultaneous acquisition and perfectly coregistered subtraction is used, and whether imaging is performed at 1 or 2 times after administration of the radiopharmaceuticals (1,3–12). The literature suggests that pinhole collimation is superior to parallel-hole collimation (7), that SPECT/CT is superior to SPECT alone (1,5,6), that dual-radiopharmaceutical imaging with simultaneous acquisition and perfectly coregistered subtraction is superior to single radiopharmaceutical imaging (1,3,4,7), and that imaging can be performed at only 1 time point without any loss in accuracy (3,4).

Before obtaining a SPECT/CT machine, our parathyroid imaging protocol consisted of single-time-point simultaneous acquisition of images with pinhole collimation in the anterior and bilateral anterior oblique projections with good results (4). When we acquired a SPECT/CT machine, we wanted the anatomic information provided by SPECT/CT but were reluctant to give up the high-resolution pinhole images, so we added SPECT/CT imaging to our existing pinhole protocol.

A recent study by Tunninen et al. compared single-time-point simultaneous acquisition of 99mTc-sestamibi and 123I images with pinhole collimation and perfectly coregistered subtraction with single-time-point simultaneous acquisition

of ^{99m}Tc-sestamibi and ^{123}I images with SPECT/CT and perfectly coregistered subtraction (3). They found no significant difference in the ability of the 2 protocols to detect and localize parathyroid adenomas. However, their pinhole protocol did not include anterior oblique images, and no comparison was made to a combined protocol that included both pinhole imaging and SPECT/CT.

Because of the length of time required to complete our combined protocol, the present investigation was undertaken to determine whether either the protocol based on pinhole collimation or the protocol based on SPECT/CT could replace the combined protocol that included both pinhole and SPECT/CT imaging. The images for all 3 protocols were derived from a single study in each patient so that the comparisons were performed on an intrapatient and intrastudy basis.

MATERIALS AND METHODS

Patient Accrual

Patient accrual began in October 2010, when SPECT/CT imaging was added to our parathyroid imaging protocol, and ended in November 2012. All patients were required to have biochemical evidence of hyperparathyroidism based on inappropriately high blood calcium and parathormone levels and to have undergone parathyroid surgery. Only patients with hyperparathyroidism secondary to 1 or more adenomas were included; patients with hyperplasia or parathyroid carcinoma were excluded. The local institutional review board approved this retrospective imaging study, and the requirement to obtain informed consent for included patients was waived.

Image Acquisition Protocol

Patients were initially asked to fast 2 h before imaging. As per our protocol, patients were first given 22.2 MBq (600 μCi) of ^{123}I orally. Two hours later, the patients were then given 925 MBq (25 mCi) of ^{99m}Tc-sestamibi intravenously. Fifteen minutes after administration of the ^{99m}Tc-sestamibi, imaging was begun. Anterior and 45° anterior oblique images were acquired for 5 min each with a pinhole collimator fitted with a 4-mm insert. Approximately 150,000 counts were acquired for the ^{99m}Tc-sestamibi and 15,000 counts for the ^{123}I. Then an anterior image of the neck and upper chest was acquired for 5 min with a low-energy high-resolution parallel-hole collimator. The images were acquired with an E.CAM γ-camera with an energy resolution of 9% (Siemens Medical Solutions).

At approximately 45 min after administration of the ^{99m}Tc-sestamibi, SPECT and CT images (CT protocol settings, 110 mAs; kV 110) were acquired of the neck and upper chest with low-energy high-resolution parallel-hole collimators. The images were acquired in a step-and-shoot mode, a noncircular orbit with 32 stops for a total of 64 views (dual-head γ-camera) over 180°, and 30 s per projection. The images were acquired with a Symbia SPECT/CT machine with an energy resolution of 9% (Siemens Medical Solutions). The radiation dose for an adult patient is estimated at 0.2 mSv for the ^{123}I protocol, 8.3 mSv for the ^{99m}Tc-sestamibi protocol, and 1.2 mSv for the SPECT/CT. This gives a total estimated procedure dose of 9.7 mSv.

For both the planar and the SPECT image acquisitions, the ^{123}I and ^{99m}Tc-sestamibi images were acquired simultaneously with an 8% symmetric energy window centered at 159 keV for ^{123}I and a 12% energy window centered at 140 keV for ^{99m}Tc-sestamibi.

This simultaneous acquisition produced perfectly coregistered ^{123}I and ^{99m}Tc-sestamibi images.

Image Processing

Subtraction images were constructed for all pairs of ^{123}I and ^{99m}Tc-sestamibi pinhole and parallel-hole images. There was no correction for cross talk. The subtractions were done manually by increasing the amount of subtraction of the ^{123}I thyroid image from the ^{99m}Tc-sestamibi image until the thyroid was essentially no longer visible (4,7). The CT images were used to correct the SPECT images for attenuation correction.

The images from each parathyroid imaging study in each patient were used to create 3 image sets: dual-radiopharmaceutical pinhole images with simultaneous acquisition and perfectly coregistered subtraction images, dual-radiopharmaceutical SPECT/CT images with simultaneous acquisition and perfectly coregistered subtraction images, and a combination of the first and second protocols. All image sets included a large-field-of-view parallel-hole image of the neck and upper chest.

Image Interpretation

Two board-certified nuclear medicine physicians independently interpreted the 3 protocols for each study in order of increasing complexity: first the pinhole image protocol, then the SPECT/CT images, and finally both together. The nonsubtracted SPECT/CT images for each patient were provided to both the interpreters, and these were reviewed if an adenoma was not identified on planar or subtracted SPECT/CT images. The interpreting physicians were masked to all patient identification, and the sequence of studies within each protocol was randomized. There was at least 1 mo between the interpretations of each of the 3 protocols for each observer.

The location of each possible adenoma was evaluated in 2 ways. In all 3 protocols, the location of any adenoma was determined with respect to side—that is, right or left—and with respect to the thyroid lobes—that is, superior, mid, or inferior. This determination was compared with the location described in the surgical report.

In addition, in the protocols that included SPECT/CT images each adenoma was localized relative to the anterior aspect of the cricoid cartilage in 3 orthogonal directions. This determination is of interest because the location of the parathyroid adenoma relative to the cricoid cartilage does not change with flexion of the neck, unlike the suprasternal notch. Thus, at the time of surgery and before making the incision the surgeon can palpate the cricoid, measure inferiorly along the skin in the midline, and then laterally, left or right, by the amounts determined from the CT images. This information can potentially serve as a guide for the placement of the skin incision. The third orthogonal measurement, from skin to the anterior mid surface of the adenoma, can potentially be used as a guide to the depth of the required dissection. In this study, the surgeons did not record a corresponding description at the time of surgery so the operative findings could not be used as a reference standard. However, this parameter was evaluated in both the SPECT/CT protocol and the combined protocol. These measurements were used to evaluate the intra- and interobserver reproducibility of each of the 3 orthogonal measurements in the CT images.

If more than 1 parathyroid adenoma was identified in an image set, the evaluation process was repeated for each additional adenoma. If an observer identified an incorrect location (false-positive) and did not grade the correct location, the correct location was assigned a zero.

Surgery

Operations included minimally invasive parathyroidectomy, unilateral exploration, bilateral exploration, hemithyroidectomy, and near-total thyroidectomy as indicated. Intraoperative assays of serum parathyroid hormone were done at the beginning of surgery and after the removal of each parathyroid gland. An intraoperative decrease in blood parathyroid hormone level of 50% or more was considered evidence of curative surgery. Intraoperative histopathologic analysis by frozen section was performed as indicated.

Pathologic Diagnosis

The diagnosis of parathyroid adenoma was based primarily on the presence of hypercellularity in conjunction with the number of abnormal parathyroid glands.

Statistical Analysis

Accuracy, the primary outcome, was defined as the proportion of locations of parathyroid adenomas that were correctly identified. The site location was coded as correct if the observer's response matched the surgical result exactly or within half the distance between the inferior and superior pole to allow for variation in the accuracy of the surgical description (4).

In addition, there were cases in which the images showed an inferior parathyroid adenoma, but the surgeon described a superior parathyroid adenoma in conjunction with a normal inferior parathyroid gland on the same side. Thus, these were superior parathyroid adenomas that were ectopically located in the posterior inferior neck. These localizations were counted as correct (4,10).

Specificity is difficult to calculate because the observers knew that each patient had at least 1 adenoma. In addition, it is considered good practice in the interpretation of parathyroid imaging studies to mention possible secondary adenomas in case there are multiple adenomas (1). At the time of surgery, if the serum parathormone level does not decrease by 50% after removal of the first adenoma, the surgeon then has a guide to the location of a likely second adenoma. However, the number of false-positive localizations was determined for each observer for the 3 protocols and served as an indicator of specificity.

The accuracy of the 3 protocols was compared statistically using a pseudo-likelihood estimate for the 4 pairwise differences between the 3 protocols (pinhole, SPECT/CT, and pinhole plus SPECT/CT) in a repeated-measures model for the binary outcome (13). Observer and protocol were entered as main effects; patient was designated as a repeated effect. Descriptive statistics for the number of lesions located, the sensitivity rate, and its 95% binomial confidence interval were also computed. A similar model was used to evaluate the certainty score (0, 1, 2, or 3) in a multinomial model for the ordered responses (13). Again, observer and protocol were entered as main effects; patient was designated as a repeated effect. A P value of less than 0.05 was considered significant.

Intraclass correlation coefficients were calculated to capture the agreement between observers and actual pathology. Fleiss recommends that intraclass correlation coefficient values greater than 0.75 represent excellent reliability and values between 0.40 and 0.75 represent fair to good reliability (14). All analyses were performed using SAS 9.3 (SAS Institute).

RESULTS

Patient Data

Fifty-nine patients with 1 or more surgically proven adenomas who underwent preoperative parathyroid imaging formed the study database. There were 47 women and 12 men. The average age for women was 56.2 y (range, 19–79 y), and for men it was 55.4 y (range, 21–73 y). For all 59 patients, the average blood calcium level was 11.1 mg/dL (range, 8.9–15.7 mg/dL), and the average serum parathormone level, at the time of surgery, was 145.2 pg/mL (range, 27–997 pg/mL).

Eleven patients were undergoing thyroid hormone replacement therapy but had not had previous thyroid or parathyroid surgery, 5 patients were undergoing thyroid hormone replacement therapy and had had previous thyroid or parathyroid surgery, and 3 had had previous thyroid or parathyroid surgery but were not undergoing thyroid hormone replacement therapy.

Surgical Results

Fifty-seven patients had 1 parathyroid adenoma and 2 patients had 2 adenomas for a total of 61 adenomas. Three patients had intrathyroidal parathyroid adenomas, 6 had a hemithyroidectomy (including the 3 with intrathyroidal parathyroid adenomas), 2 had a subtotal thyroidectomy, and 1 had thyroid remnant resection. Eight patients had ectopic parathyroid adenomas away from the thyroid. Of these, 3 patients had a parathyroid adenoma in the mid mediastinum and 5 had parathyroid adenomas in the superior thymus.

The average initial intraoperative parathyroid hormone level was 145.2 pg/mL (range, 27–997 pg/mL), and the average final postresection intraoperative parathyroid hormone level was 30.8 pg/mL (range, 6–74 pg/mL). The average percentage decrease in the intraoperative parathyroid hormone level from preresection to postresection was 75.0% (range, 42%–94%).

Pathologic Findings

Histology confirmed hypercellular parathyroid tissue in all resected glands. The average weight of the adenomas was 0.80 g (range, 0.02–5.00 g).

Protocol Analysis

The interpretation results on a per-adenoma basis for the 2 observers individually and combined are shown in Table 1. In the evaluation of all 3 protocols, observer A tended to have a lower sensitivity and lower false-positive rate than observer B. The interpretation results when the degree of certainty grades 1 through 3 were combined on a per-adenoma basis for the observers individually and combined are shown in Table 2. There were more true-positive and fewer false-negative results with the pinhole protocol than with SPECT/CT protocol ($P = 0.002$). Figure 1 shows the number of adenomas that were localized correctly (true-positives), mislocalized (false-positives), and undetected (false-negatives).

Table 3 shows the results of a direct comparison of the pinhole and SPECT/CT protocols for all adenomas that were visualized by both observers. Observer A rated the pinhole protocol superior to the SPECT/CT protocol 42% to 9% of the time and the 2 equal 49% of the time (Figs. 2

Protocol*	Degree of certainty of location			
	0	1	2	3
Pinhole				
Observer A	11	8 (2)	20 (1)	22 (1)
Observer B	4	9 (10)	17 (2)	31 (1)
Average	7.5	8.5 (6)	18.5 (1.5)	26.5 (1)
SPECT/CT				
Observer A	21	7 (1)	8	25
Observer B	17	4 (1)	13 (1)	27 (2)
Average	19	5.5 (1)	10.5 (0.5)	26 (1)
Pinhole + SPECT/CT				
Observer A	17	5 (1)	10 (1)	29
Observer B	5	9 (6)	14 (4)	33
Average	11	7 (3.5)	12 (2.5)	31

*Both pinhole and SPECT/CT protocols involved dual-tracer simultaneous acquisition with subtraction.

0= no adenomas seen; 1 = possible adenoma; 2 = probable adenoma; 3 = definite adenoma.

Numbers in parentheses indicate number of localizations that were incorrect (false-positives).

and 3). Observer B rated the SPECT/CT protocol superior to the pinhole protocol 34% to 26% of the time and the 2 equal 40% of the time (Figs. 4 and 5). In the 5 adenomas in which both observers rated either the pinhole or the SPECT/CT protocol over the other, observer A always favored the pinhole protocol and observer B always favored the SPECT/CT protocol. In general, the concordance between the 2 observers was relatively poor, suggesting differences in personal preferences for the pinhole and SPECT/CT protocols.

Protocol*	Localization success		
	Adenomas	Correct	95% CI
Pinhole			
Observer A	50/61	82%	73–91
Observer B	57/61	93%	90–99
Average	53.5/61	88%	84–92
SPECT/CT			
Observer A	40/61	66%	54–78
Observer B	44/61	72%	61–83
Average	42/61	69%	63–75
Pinhole + SPECT/CT			
Observer A	43/61	70%	64–76
Observer B	56/61	92%	89–95
Average	49.5/61	81%	76–86

*Both pinhole and SPECT/CT protocols involved dual-tracer simultaneous acquisition with subtraction.

CI = exact binomial confidence interval.

Calculations are on per-adenoma basis. There were 61 adenomas in 59 patients.

Localization Relative to Cricoid

The intraclass correlation coefficients for observer A and B for the midline measurement from the anterior cricoid cartilage inferiorly to the level of the adenoma were 0.91 and 0.76, respectively; for the measurement from the midline laterally to skin directly anterior to the adenoma, they were 0.78 and 0.56, respectively; and for the measurement from the skin posteriorly to the anterior mid surface of the adenoma, they were 0.92 and 0.93, respectively. The interobserver correlation coefficients for observer A and B for the first and second midline measurements from the anterior cricoid inferiorly to the level of the adenoma were 0.91 and 0.79, respectively; for the first and second measurements from the midline laterally to skin directly anterior to the adenoma, they were 0.64 and 0.44, respectively; and for the first and second measurements from the skin posteriorly to the anterior mid surface of the adenoma, they were 0.90 and 0.88, respectively. In general, the intra- and interreproducibility were better for the measurements from the cricoid to the level of the adenoma and from the skin to the anterior mid surface of the adenoma than for the measurement from the midline laterally to the skin directly anterior to the adenoma.

DISCUSSION

This retrospective study compared 3 state-of-the-art protocols for parathyroid imaging: single-time-point simultaneous acquisition of ^{99m}Tc-sestamibi and ^{123}I images with pinhole collimation in the anterior and bilateral anterior oblique projections with perfectly coregistered subtraction, single-time-point simultaneous acquisition of ^{99m}Tc-sestamibi and ^{123}I images with SPECT/CT with perfectly coregistered subtraction, and the combination of the first 2 protocols. The results demonstrate a higher true-positive localization rate for the pinhole protocol than the SPECT/CT protocol and a lower false-negative rate for the pinhole protocol than either the SPECT/CT protocol or the combined protocol. In addition,
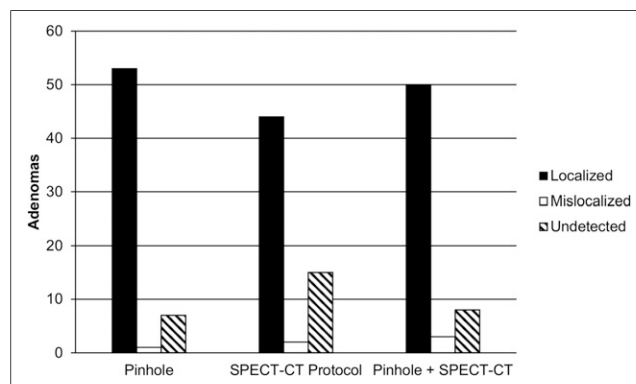

FIGURE 1. Performance of each of 3 protocols is shown for localizing 61 parathyroid adenomas in 59 patients. Data represent average of results for 2 observers. All 3 protocols included perfectly coregistered subtraction images created by subtracting ^{123}I images from ^{99m}Tc-sestamibi images, plus anterior parallel-hole collimator image of neck and upper chest.

TABLE 3
Direct Comparison of Pinhole and SPECT/CT Protocols

| Observer | Protocol rating | | |
	Pinhole better	SPECT/CT better	Equal
A	19 (42%)	4 (9%)	22 (49%)
B	14 (26%)	20 (34%)	23 (40%)

satisfactory intra- and interobserver reproducibility of a novel method for localizing a parathyroid adenoma relative to the cricoid cartilage using the CT images in the SPECT/CT and combined protocols was demonstrated. This localization method may assist the endocrine surgeon in selecting the site of incision when performing minimally invasive surgery.

There are advantages and disadvantages among the 3 parathyroid imaging protocols. The pinhole protocol has the highest spatial resolution because of the physics of pinhole collimation and the ability to place the collimator at an optimal, relatively short, distance from the structures of interest without interference from patient anatomy. However, the 3-view pinhole images give limited 3-dimensional information, and the images cannot be coregistered with CT images for anatomic correlation.

The SPECT/CT protocol has the ability to coregister functional and anatomic images, and the tomographic images give optimal 3-dimensional information. However, the SPECT images are reconstructed from a series of planar images acquired with a parallel-hole collimator. The spatial resolution of the parallel-hole collimator images is less than the pinhole
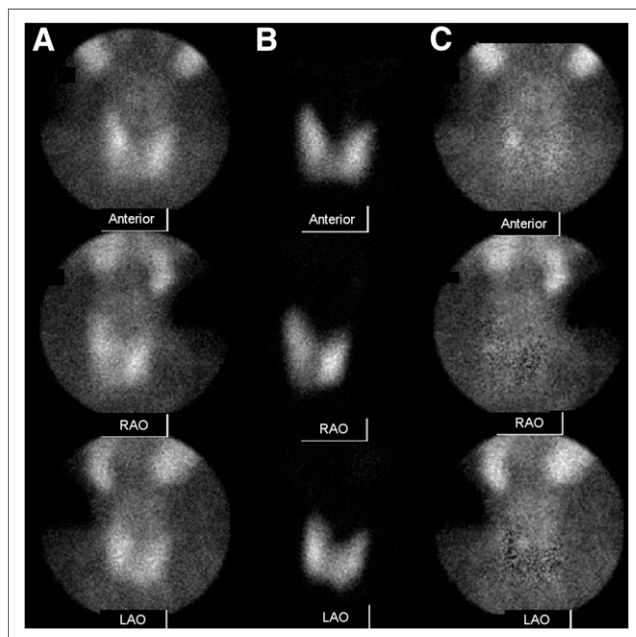
collimator images because of the physics of parallel collimation and the inability to place the parallel-hole collimator close to the structures of interest secondary to interference from the patients face, chest, and shoulders.

The combined protocol preserves the advantages of both the pinhole and the SPECT protocols and adds the synergistic ability to detect a possible parathyroid adenoma in the high-resolution pinhole images, identify the same activity in the SPECT images, and then correlate the functional abnormality with the coregistered CT images of anatomy. On the other hand, the combined protocol requires a relatively long acquisition time that is inconvenient for both the patient and the nuclear medicine department.

High-resolution coregistered CT images of anatomy have several advantages in parathyroid imaging studies. The CT images can be used to precisely localize most parathyroid adenomas; measure the size of the adenoma; localize the adenoma relative to other structures of interest such as the cricoid cartilage; evaluate the thyroid for nodules, which
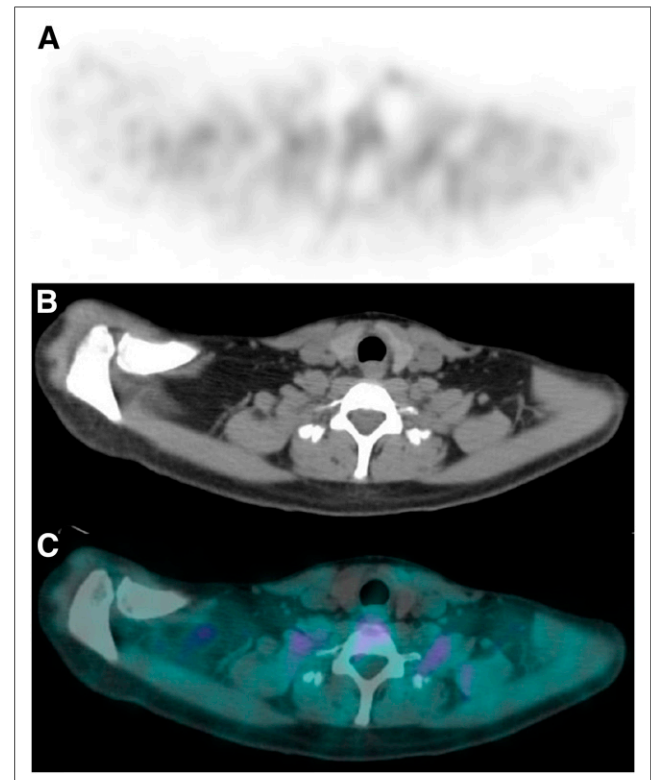
FIGURE 3. Selected perfectly coregistered subtraction SPECT image (A), corresponding CT image (B), and fused image (C) from SPECT/CT protocol. None of the maximum-intensity-projection images are shown. No focus of postsubtraction activity was seen in any image. Both observers scored this image set as 0—that is, no adenoma seen. However, in the CT image there is small low-density structure along posterior aspect of right lobe of thyroid consistent with location of focus of activity in pinhole protocol images. Surgery confirmed right superior parathyroid adenoma. This is an example of parathyroid adenoma that was better seen in pinhole protocol than in SPECT/CT protocol.
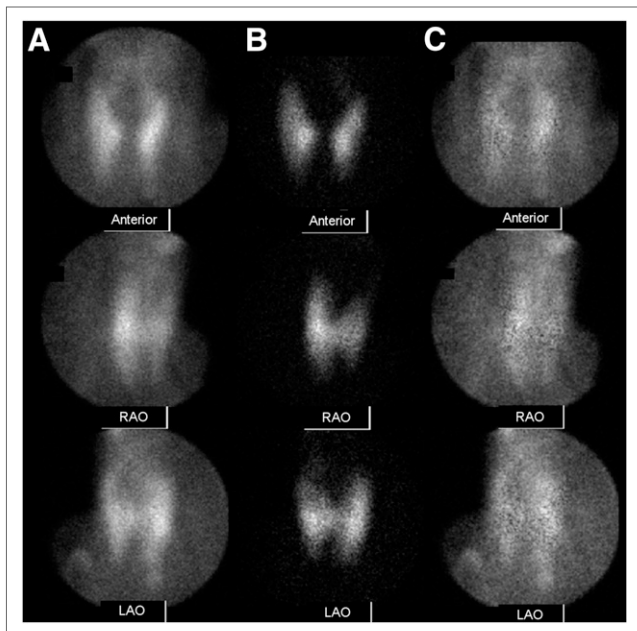
FIGURE 2. Anterior and anterior oblique pinhole images for ^{99m}Tc-sestamibi (A), ^{123}I (B), and subtraction images (C) from pinhole protocol. Subtraction images show persistent focus of activity consistent with parathyroid adenoma just posterior to mid to superior pole of right lobe of thyroid. Both observers scored this finding as 2—that is, a probable adenoma.

FIGURE 4. Anterior and anterior oblique pinhole images for ^{99m}Tc-sestamibi (A), ^{123}I (B), and subtraction images (C) from pinhole protocol. Subtraction images show possible mild focus of activity consistent with parathyroid adenoma just inferior to inferior pole of left lobe of thyroid. The 2 observers scored this finding as 1 and 0—that is, possible adenoma and no adenoma seen.

may retain ^{99m}Tc-sestamibi and be confused with a parathyroid adenoma; and perform attenuation correction on the SPECT images. Consequently, it would be difficult for those who have used SPECT/CT for parathyroid imaging to give up the CT images.

In a recent study by Tunninen et al., they compared 5 different parathyroid imaging protocols including a pinhole protocol and SPECT/CT protocol similar to the ones evaluated here (*3*). However, their pinhole protocol did not include anterior oblique images, and no comparison was made to a combination of the pinhole and SPECT/CT protocols. Anterior oblique pinhole images have been shown to increase the accuracy of the parathyroid imaging study (*15*), and the combined protocol has none of the tradeoffs that the pinhole and SPECT/CT protocols have individually. Tunninen et al. found no significant difference in the ability of the 2 protocols to detect and localize parathyroid adenomas although there was a tendency for the pinhole protocol to identify more parathyroid adenomas than the SPECT/CT protocol. The pinhole protocol was begun at 15 min and the SPECT/CT protocol was begun secondarily at 45 min, similar to the time sequence in the present study.

It is known that there is relatively rapid washout of ^{99m}Tc-sestamibi from approximately 20% of parathyroid adenomas, and this phenomenon may decrease the localization accuracy of the SPECT/CT protocol relative to the pinhole protocol when it is performed secondarily as it was here (*1,4,16,17*). In addition, the SPECT images of the SPECT/CT protocol

are reconstructed from parallel-hole collimation images whose spatial resolution is less than the pinhole collimation images of the pinhole protocol and this fact may contribute to a lower localization accuracy of the SPECT/CT protocol relative to the pinhole protocol (*7*). Additionally, this study does not address the relative accuracy of other SPECT/CT protocols, for example, single-isotope dual-time-point imaging at 15 and 90 min, that also currently exist in clinical practice.

The main limitation of the current study is the lack of randomization of the sequence of pinhole and SPECT/CT protocols. We are unaware of any study that has compared the pinhole protocol with the SPECT/CT protocol as performed here with the SPECT/CT images acquired first. There appears to be a need for a direct comparison of the pinhole protocol and the SPECT/CT protocol with the SPECT/CT protocol performed either first or in a randomized order. Randomization could address the question of
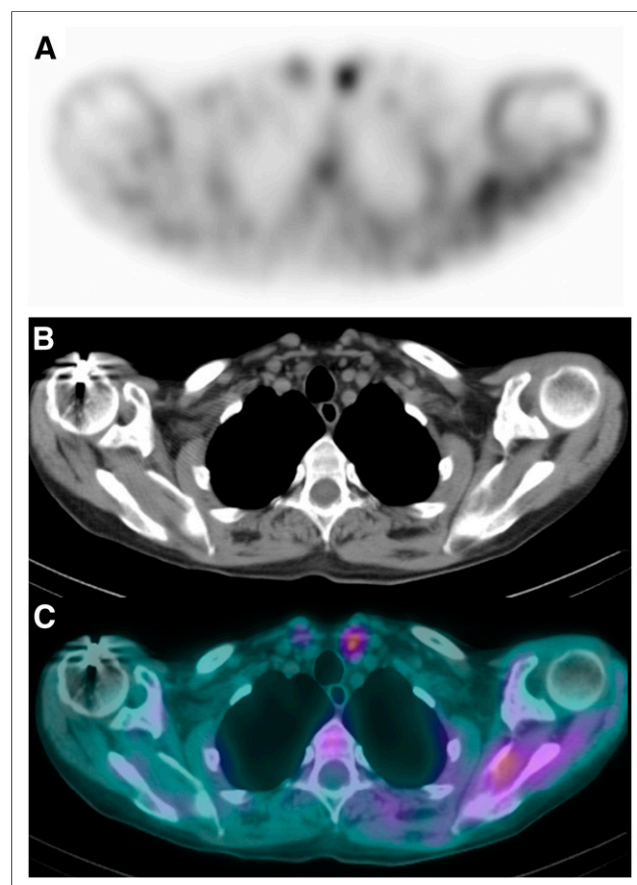

FIGURE 5. Selected perfectly coregistered subtraction SPECT image (A), corresponding CT image (B), and fused image (C) from SPECT/CT protocol. None of the maximum-intensity-projection images are shown. Focus of postsubtraction activity was seen inferior to inferior tip of left thyroid. The 2 observers scored this finding as 3 and 2—that is, definite adenoma and probable adenoma. Surgery revealed ectopic parathyroid adenoma in superior left thymus. This is an example of parathyroid adenoma that was better seen in SPECT/CT protocol than in pinhole protocol. Patient had had 2 previous right parathyroidectomies.

whether SPECT/CT subtraction at 45 min is best compared with an earlier time point.

In addition, washout of ^{99m}Tc-sestamibi from some parathyroid adenomas or lower spatial resolution in the SPECT/CT images might explain why the combined protocol did not perform better than the pinhole protocol. That is, in the combined protocol the observers may have been reluctant to diagnose a focus of faint activity seen in the pinhole images as an adenoma if it was not confirmed in the SPECT images.

Recently, several papers have reported the use of contrast enhanced 4D CT of the neck and upper chest for localization of parathyroid adenomas (18–20). The term 4D refers to 3 spatial dimensions plus the time dimension. The time dimension reflects the fact that CT images are acquired at 2 or 3 times during the study, once before administration of intravenous CT contrast and once or twice afterward. A localization success rate as high as 90% has been reported (17). The use of intravenous contrast could be added to the SPECT/CT protocol.

CONCLUSION

The pinhole protocol correctly detected and localized more adenomas than the SPECT/CT protocol and missed fewer adenomas than either the SPECT/CT protocol or the combined pinhole and SPECT/CT protocols. The fact that the pinhole protocol was acquired before the SPECT/CT protocol may have influenced both of these findings. However, the superior spatial resolution of the pinhole collimator is at least partially responsible for the improved accuracy. A comparison in which SPECT/CT is acquired before pinhole imaging is probably warranted. In general, the SPECT/CT protocol has the advantage of providing superior anatomic information.

DISCLOSURE

ACKNOWLEDGMENTS

REFERENCES

1. Mullan BP. Nuclear medicine imaging of the parathyroid. *Otolaryngol Clin North Am.* 2004;37:909–939.
2. Doberry GM, Wells SA. Parathyroid glands. In: Townsend CM, Beauchamp R, Evers BM, Mattox KL, eds. *Sabiston Textbook of Surgery*: *The Biological Basis of Modern Surgical Practice*. 18th ed. Philadelphia, PA: Saunders Elsevier; 2008.
3. Tunninen V, Varjo P, Schildt J, et al. Comparison of five parathyroid scintigraphic protocols. *International J Mol Imaging.* 2013;2013:1–12.
4. Caveny SA, Klingensmith WC III, Martin WE, et al. Parathyroid imaging: the importance of dual-radiopharmaceutical simultaneous acquisition with ^{99m}Tc-sestamibi and ^{123}I. *J Nucl Med Technol.* 2012;40:104–110.
5. Neumann DR, Obuchowski NA, DiFilippo FP. Preoperative I-123/Tc-99m-sestamibi subtraction SPECT and SPECT-CT in primary hyperparathyroidism. *J Nucl Med.* 2008;49:2012–2017.
6. Lavely WC, Goetze S, Friedman KP, et al. Comparison of SPECT-CT, SPECT, and planar imaging with single- and dual-phase Tc-99m-sestamibi parathyroid scintigraphy. *J Nucl Med.* 2007;48:1084–1089.
7. Klingensmith WC, Koo PJ, Summerlin A, et al. Parathyroid imaging: the importance of pinhole collimation with both single- and dual-tracer acquisition. *J Nucl Med Technol.* 2013;41:99–104.
8. Harris L, Yoo J, Driedger A, et al. Accuracy of technetium-99m SPECT-CT hybrid images in predicting the precise intraoperative anatomical location of parathyroid adenomas. *Head Neck.* 2008;30:509–517.
9. Nichols KJ, Tomas MB, Tronco GG, et al. Preoperative parathyroid scintigraphic lesion localization: Accuracy of various types of readings. *Radiology.* 2008;248:221–232.
10. Eslamy HK, Ziessman HA. Parathyroid scintigraphy in patients with primary hyperparathyroidism: Tc-99m-sestamibi SPECT and SPECT-CT. *Radiographics.* 2008;28:1461–1476.
11. Greenspan BS, Dillehay G, Intenzo C, et al. SNM practice guideline for parathyroid scintigraphy 4.0. *J Nucl Med Technol.* 2012;40:111–118.
12. Hindié E, Ugur O, Fuster D, et al. 2009 EANM parathyroid guidelines. *Eur J Nucl Med Mol Imaging.* 2009;36:1201–1216.
13. Liang KY, Zeger SL. Longitudinal data analysis using generalized linear models. *Biometrika.* 1986;73:13–22.
14. Fleiss JL. Reliability of measurement. In: *The Design and Analysis of Clinical Experiments*. New York, NY: John Wiley Sons; 1986:1–31
15. Ho Shon IA, Bernard E, Roach P, et al. The value of oblique pinhole images in pre-operative localization with Tc-99m-sestamibi for primary hyperparathyroidism. *Eur J Nucl Med.* 2001;28:736–742.
16. Kulkarni KP, Van Nostrand D, Wells K, et al. The frequency of parathyroid adenomas and/or hyperplasia that have washout equal to normal thyroid tissue in patients who have a negative dual time point Tc-99m-sestamibi scan [abstract]. *J Nucl Med.* 2010;51:56P–57P.
17. Doumas A, Iakovou I, Boundas D, et al. How often are parathyroid adenomas expressing the same Tc-99m-washout compare to adjacent thyroid parenchyma? *Eur J Nucl Med Mol Imaging.* 2009;36:S449.
18. Chazen JL, Gupta A, Dunning A, et al. Diagnostic accuracy of 4D-CT for parathyroid adenomas and hyperplasia. *Am J Neuroradiol.* 2012;33:429–433.
19. Beland MD, Mayo-Smith WW, Grand DJ, et al. Dynamic MDCT for localization of occult parathyroid adenomas in 26 patients with primary hyperparathyroidism. *AJR.* 2011;196:61–65.
20. Beland MD, Monchik JM. 4D CT: A diagnostic tool to localize an occult parathyroid adenoma in a patient with primary hyperparathyroidism. *Med Health R I.* 2012;95:157–158.